A MODEL FOR THE ORIGIN OF ANISOTROPIC GRAIN BOUNDARY CHARACTER DISTRIBUTIONS IN POLYCRYSTALLINE MATERIALS

Gregory S. Rohrer, Jason Gruber, and Anthony D. Rollett.
Department of Materials Science and Engineering,
Carnegie Mellon University
Pittsburgh PA, 15213

ABSTRACT

A model is described for the development of anisotropic grain boundary character distributions from initially random distributions. The model is based on biased topological changes in the grain boundary network that eliminate and create boundaries during grain growth. The grain boundary energy influences the rates of these topological changes by altering the relative areas of the interfaces. The model predicts grain boundary character distributions that are inversely related to the grain boundary energy and are consistent with experimental observations.

INTRODUCTION

The grain boundary character distribution (GBCD) is defined as the relative areas of grain boundaries as a function of lattice misorientation and grain boundary orientation. It can be considered as an expansion to higher dimension space of the misorientation distribution function (MDF) and is typically normalized to give units of multiples of a random distribution (MRD). It has recently been observed in experiments and in simulations that the GBCD, even in an otherwise untextured polycrystal, is anisotropic [1]. The results indicate that the most common boundaries in anisotropic distributions have greater average areas than the less common boundaries and that there is a higher incidence of these boundaries [2]. Peaks in anisotropic distributions commonly reach values of 5 to 10 MRD and, even in a relatively isotropic material (Al), peaks in excess of 3 MRD are commonly observed [3]. Furthermore, based on the results of experiments [4,5] and computer simulations in two and three dimensions [6-10], the GBCD is inversely correlated to the grain boundary energy. The only available comprehensive experimental data indicates that the logarithm of the population is approximately linear with the energy, which is consistent with the results of a three-dimensional computer simulation [6, 10, 11]. These results are compared in Fig. 1.

Holm et al. [6] were the first to propose a mechanism for the enhanced areas of low energy grain boundaries. Assuming the grain boundaries in Fig. 2a have the same lengths (L_1=L_2) and energies (γ_1 and γ_2), then the dihedral angle, Ψ, is $2\pi/3$. If the energies change so that $\gamma_1 < \gamma_2$, then the dihedral angle will increase, L_1 will increase by the amount ΔL_1, and L_2 will decrease. This lengthening and shortening of boundaries enhances the relative areas of low energy grain boundaries. The alteration of grain boundary lengths in a two-dimensional network was also recently used as the basis for a model to study the spatial correlation among high energy grain boundaries [12]. However, this mechanism does not, by itself, explain why low energy grain boundaries occur in greater numbers.

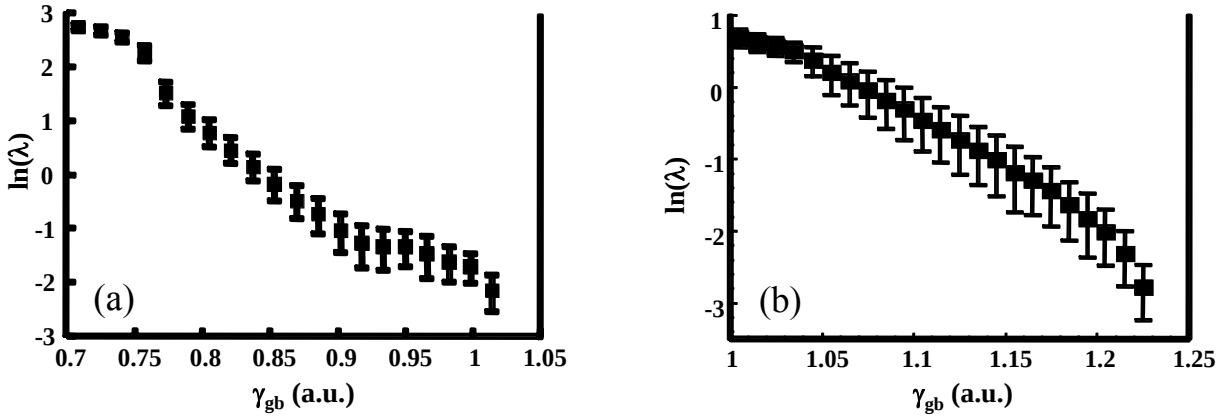

Figure 1. Correlation between the logarithm of the grain boundary population, measured in MRD units, and the grain boundary energy. (a) experimental results from measurements of polycrystalline MgO [5]. At each energy, the square is the mean population and the error bars show the standard deviation. (b) Simulated results from Grain 3D [10].

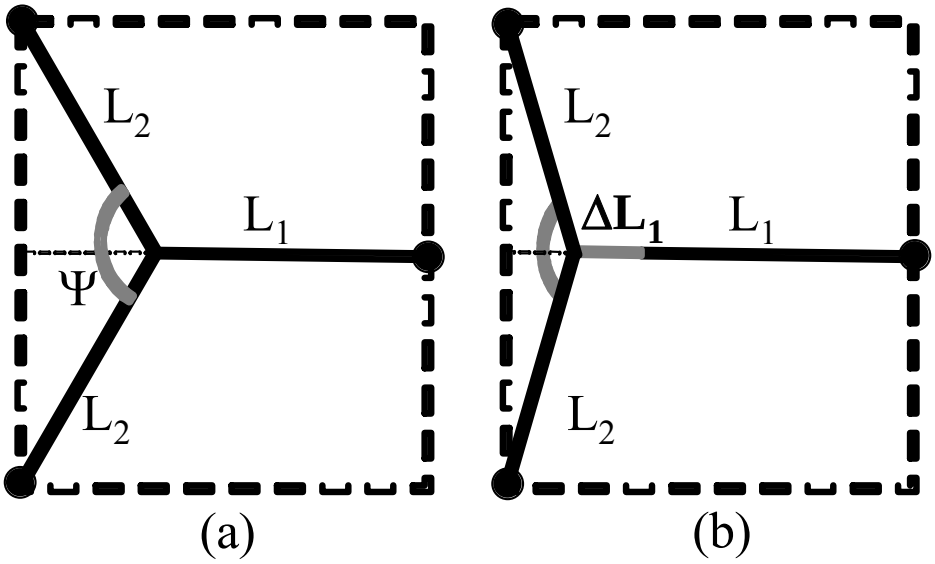

Figure 2. Triple junctions for the case of (a) three equal energy grain boundaries and (b) when the horizontal grain boundary has a lower energy. It is assumed that the grain boundary line segments are fixed at the circles at edges of the box.

The purpose of this paper is to describe a model for the formation of anisotropic GBCDs from initially random GBCDs during normal grain growth. Using the observation that a grain boundary's energy is inversely related to its area, the model for the evolution of the distribution assumes that the rates at which grain boundaries are eliminated are inversely proportional to the grain boundary areas, and, therefore, directly proportional to the grain boundary energies. It is shown that the model reproduces the main characteristics of the experimental results, including the observation that low energy boundaries occur in greater numbers than expected in a random distribution; based on these results, it is concluded that the assumed mechanisms are a plausible explanation for the development of anisotropic grain boundary character distributions.

THE MODEL

Overview

We begin by considering how the grain boundary energy influences the grain boundary area. With reference to the triple junctions illustrated in Fig. 2, we begin by assuming that the three grain boundaries are fixed at their endpoints and the triple junction geometry obeys Young's law for interfacial equilibrium. Under these conditions, the additional length is given by the following equation:

$$\Delta L_1 = \frac{L_1}{2}\left[1 - \frac{\sqrt{3}}{\tan\left(\cos^{-1}\left(\frac{\gamma_1}{2\gamma_2}\right)\right)}\right] \qquad (1)$$

Note that for the case of $\gamma_1 = \gamma_2$, $\Delta L_1 = 0$. As $\gamma_1 << \gamma_2$, ΔL_1 approaches $L_1/2$.

Using Eq. 1, we can estimate the influence of the boundary lengthening mechanism on the GBCD. First, assume there are just a few boundaries (say 2%) with $\gamma_1 << \gamma_2$ so that we can assume that the low energy boundary is always attached to two higher energy boundaries. All the low energy boundaries will have a length of $3L_1/2$, the high energy boundaries attached to it (4% of the total) will have lengths $\sqrt{3}L_2/2$, and the remaining 94% of boundaries in the system will have length L_1. Using these estimates, and assuming that boundary area is equal to the square of the length, the population of the low energy grain boundaries is 2.22 MRD and the population of high energy boundaries is 0.98 MRD.

Note that the estimates above are maximal, assuming a vanishingly small grain boundary energy and configurations in which the low energy boundary is always connected to two high energy boundaries. Therefore, this mechanism does not provide a plausible explanation for peaks in the GBCD that commonly exceed 3 MRD and it provides no explanation for the higher incidence of low energy boundaries. It can be concluded that boundary area changes associated with adjustments of the triple junction positions do not have a large enough effect on the areas to explain the observed anisotropies. Furthermore, this mechanism can not account for the observed anisotropic number fractions [2]. However, the lengthening mechanism should be viewed as an essential factor that contributes to the anisotropy of the GBCD. In fact, in what follows, we assume that boundary area changes are the mechanism that biases topological changes and alters the number fractions of grain boundary types.

There are several physical processes that occur during grain growth that can alter the GBCD. One process involves incremental changes in area as boundaries move. Another process is the critical events that change the topology of the network. Grain faces lose edges (and area) until they are triangular and eventually collapse. Two grains can also join and create a new triangular face. Faces are also destroyed when four-sided tetrahedral grains collapse. Note that these topological changes represent the end points of incremental motion and in what follows, we will take the topological events as proxies for positive and negative incremental area changes.

Assumptions

The model for the development of the anisotropic GBCD is based on the following assumptions:

1. The topological structure during grain growth is scale invariant. In other words, the average number of faces per grain is independent of the mean grain size. This assumption allows us to focus on the changes in the distribution of grain boundary types, without considering the dissipative loss of interfacial area. In the case of isotropic materials, three dimensional computer simulations have been used to demonstrate the scale invariance of the network topology [13]. These simulations compare favorably to results from Al, where boundary properties are naturally anisotropic [14]. Recent three dimensional grain growth simulations have verified that microstructures with anisotropic grain boundary properties remain scale invariant during grain growth [15].

2. All incremental changes in grain boundary area are represented by the appearance or disappearance of grain faces. Note that in a real situation, all grain faces are constrained to the same sequence of events: they are created, they grow, they shrink, and then they are eliminated. The present model is based on average probabilities for the events at the endpoints, without consideration of individual grain faces or the intermediate incremental changes.

3. The distribution of grain boundary types that arises from grains growing into one another is determined by the grain orientation distribution. This assumes that the pair-wise spatial configuration of orientations is random. It has been shown previously that for a fixed orientation distribution, the crystals can be positioned to exhibit non-random misorientation distributions [16]. So, while the assumption is certainly a plausible condition, there may be cases where it does not hold.

4. The probability that a grain face is eliminated is inversely proportional to its area. In other words, the smallest faces are eliminated with the highest probability. This assumption is based on observations of soap froths reported by Smith [17].

5. There is a functional relationship between grain boundary energy and grain boundary area. Recent three dimensional grain growth simulations with anisotropic properties has shown that this is the case [15]. As an approximate model for this relationship, we modify Eq. 1 and assume that the length, L_i, of the i^{th} GB, when connected to two boundaries of average length, $\overline{L}$, depends on the ratio between its own energy, γ_i, and the average energy, $\overline{\gamma}$, in the following way:

$$\frac{L_i}{\overline{L}} = 1 + \left\lfloor \frac{1}{2}\left(1 - \frac{\sqrt{3}}{\tan\left[\cos^{-1}\left(\frac{\gamma_i}{2\overline{\gamma}}\right)\right]}\right)\right\rfloor \qquad (2)$$

This expression for L_i has the property that for $\gamma_i = \overline{\gamma}$, $L_i = \overline{L}$ and as γ_i goes to 0, L_i goes to $3\overline{L}/2$. The area of the face is then given by the square of its length. Here, the average length is fixed at 1.

It should be noted that an alternate approach to determining the relationship between the energy and the area is to extract it from the results of three dimensional grain growth simulations. This approach will be discussed briefly in the results section.

With these assumptions, we can quantify the probability that, for a single critical event (e), a GB of the i^{th} type is created or destroyed. The probability that it is created is equal to fractional number of boundaries of the i^{th} type expected from the grain orientation texture. For this analysis, we assume a random grain orientation distribution. Therefore, the probability that a boundary is created is equal to its expected population in a random distribution, (ρ_i). The probability that it is destroyed is equal to the normalized product of the fractional number of boundaries of the i^{th} type and the inverse of their area ($n_i/L_i^2 = \alpha_i n_i$). Therefore, the probability that during a critical event the population of the i^{th} type of GB is changed is,

$$\frac{\Delta n_i}{\Delta e} = \left(\rho_i \quad - \quad \frac{\alpha_i n_i}{\sum_{i=1}^{N} \alpha_i n_i} \right) \quad . \tag{3}$$

Note that when summed over all grain boundaries types, the creation and annihilation terms are both equal to 1. Therefore, as critical events occur, the total number of grain boundaries under consideration is unchanged. This reflects the assumption of scale invariance.

Details of the calculations

To determine how the GBCD changes as critical events occur, we begin by assuming an initial random distribution and a functional form for the anisotropy of the grain boundary energy. Here, we consider only energy anisotropies that vary with a single crystallographic parameter. We initially consider energy functions that have a Read-Shockley like variation in the energy as a function of misorientation.

$$\begin{aligned} \gamma_i &= \frac{\theta_i}{\theta_c}\left(1 - \ln\frac{\theta_i}{\theta_c}\right) \qquad for\, \theta_i < \theta_c \\ \gamma_i &= 1 \qquad\qquad\qquad\quad for\, \theta_i > 1 \end{aligned} \tag{4}$$

In Eq. 4, θ_i is the angle that characterizes the disorientation, and θ_c is the cut-off angle beyond which the energy is constant. The energy and GBCD are discretized in 0.5° intervals and, thus, there are 125 discrete boundary types.

To test a situation that is more characteristic of variations that occur as a function of the grain boundary plane orientation at a fixed lattice misorientation, we assume the following energy anisotropy:

$$\gamma_i = 1 + \varepsilon(\sin 2\omega_i)^4 \tag{5}$$

where ω parameterizes the inclination of the grain boundary in the bicrystal reference frame. For calculations with this energy function, the misorientation is not accounted for and it is assumed that all boundaries have this energy dependence in the domain of possible inclinations.

To begin the calculation, the initial populations of grain boundaries are defined so that each occurs with a population of 1 MRD. The average energy (weighted by the population) is determined according to the following equation:

$$\bar{\gamma} = \frac{1}{N}\sum \lambda_i \gamma_i \qquad (6)$$

where N is the number of distinct boundary type2 (125) and λ_i is the population of grain boundaries of that type, measured in MRD. Using this average energy, the initial grain boundary lengths are computed according to Eq. 2. These lengths are then used to determine the weighting factors, α_i, in Eq. 3, such that $\alpha_i = 1/L_i^2$. With these initial conditions, all Δn_i are computed according to Eq. 3 and the populations, n_i, are adjusted. With the new populations, a new average energy is computed according to Eq. 6 and this value is used to calculate new values for the lengths L_i and the weighting factors α_i. The process of changing the population then repeats iteratively. After a sufficient number of iterations, a steady state is reached where all Δn_i become negligible.

RESULTS

The number fractions of grain boundaries with the minimum energy and the maximum energy are plotted as a function of the number of critical events in Fig. 3. The results show that the GBCD reaches a steady state after approximately $2x10^6$ critical events. Note that these changes in the numbers of boundaries do not account for the relative areas.

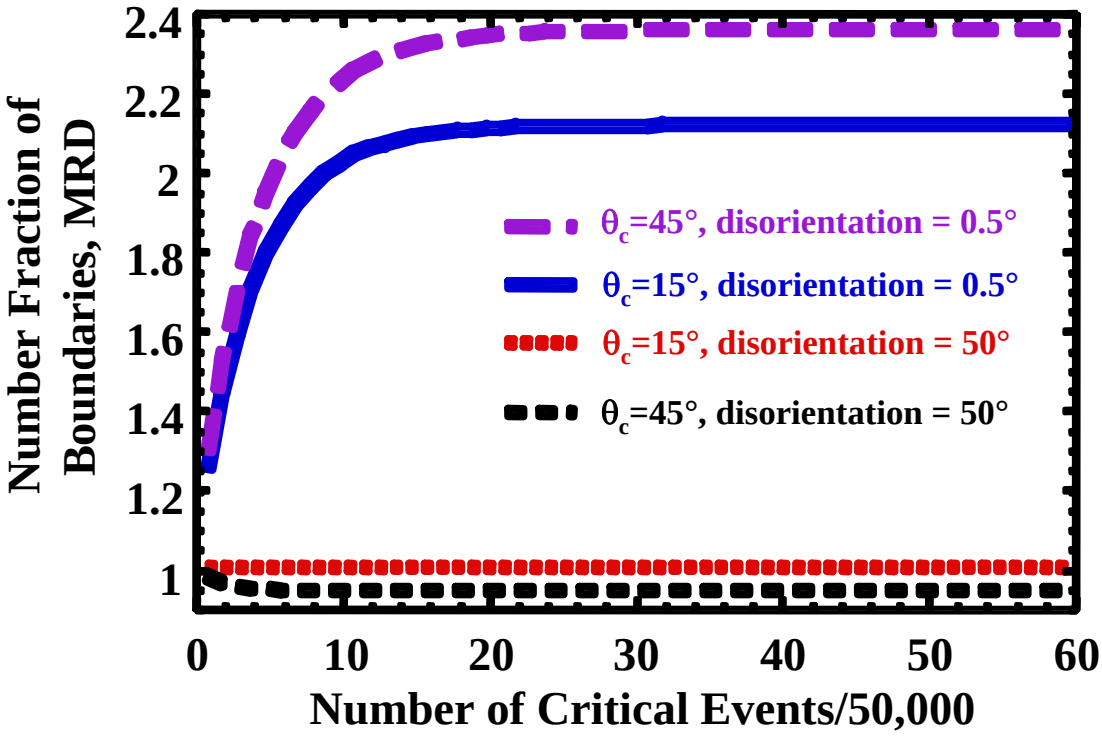

Figure 3. The number MRD values for grain boundaries number fractions in a low energy bin at 0.5° and a high energy bin at 50° as a function of the number of critical events.

The final area distributions of grain boundary types are shown in Fig. 4. The lowest energy grain boundaries have populations that are four to six times that expected in a random

distribution and the highest energy (angle) grain boundaries have populations slightly less than would be expected. The fractional area distribution that results from the energy function with a 15° cutoff overlaps with the initial random distribution throughout most of the domain.

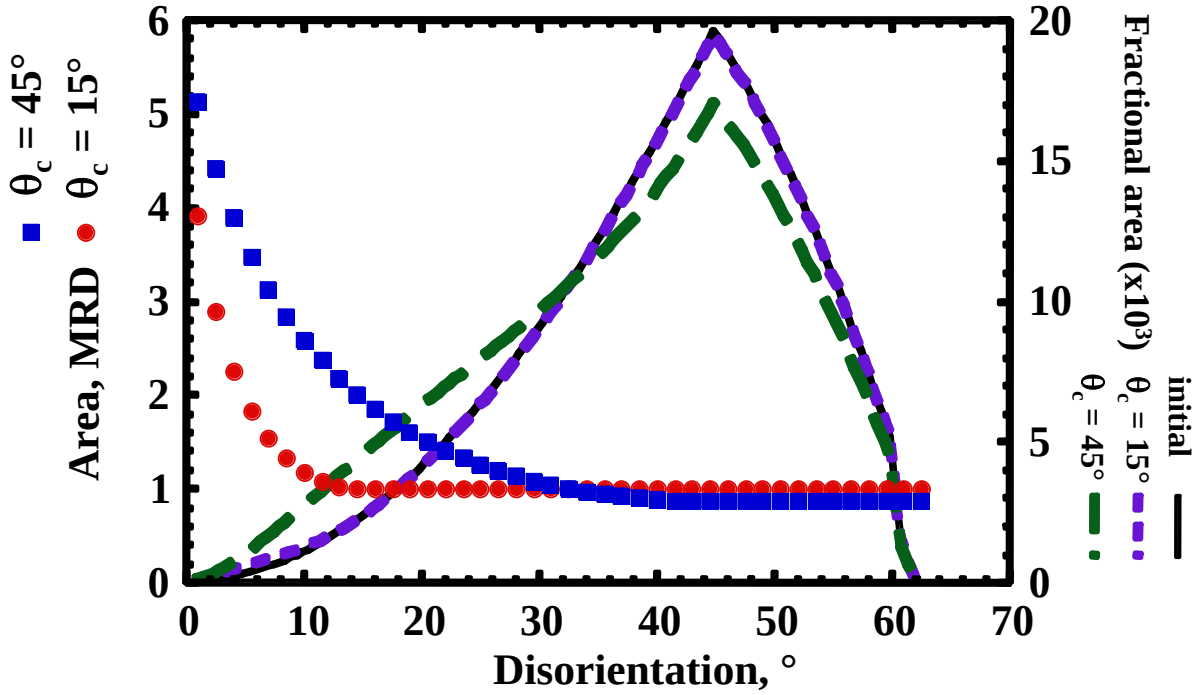

Figure 4. Steady state grain boundary character distributions resulting from two different energy functions, specified by Eq. 4. The area MRD is the area of a given grain boundary type, divided by the average area of all types. The fractional area is the area of a given grain boundary type, divided by the total grain boundary area.

As mentioned briefly in the previous section, the calculation can also be done using a fixed energy-area relationship derived from grain growth simulations. Three-dimensional Monte Carlo grain growth simulations using the same grain boundary energy anisotropy assumed in Eq. 4 have been reported [15]. The area distributions derived from the simulations are similar to those depicted in Fig. 4. The results of these simulations were used to find a relationship between the relative grain boundary areas and the relative grain boundary energies. When the coefficients of a quadratic function were fit to the simulation results, the following equation was found to be a good fit to the results:

$$A_i = 3.61 - 4.369\gamma_i + 1.729\gamma_i^2 \qquad (7)$$

Where A_i is the relative area of the i^{th} type of boundary. The weighting factors, α_i, in Eq. 3 are then $1/A_i$. The initially random population was then evolved as before, except that the weighting factors (α_i) used in Eq. 3 were constant as the population evolved. The results were qualitatively the same, yet differed in the quantitative details. Examples of distributions derived from this method are shown in Fig. 5.

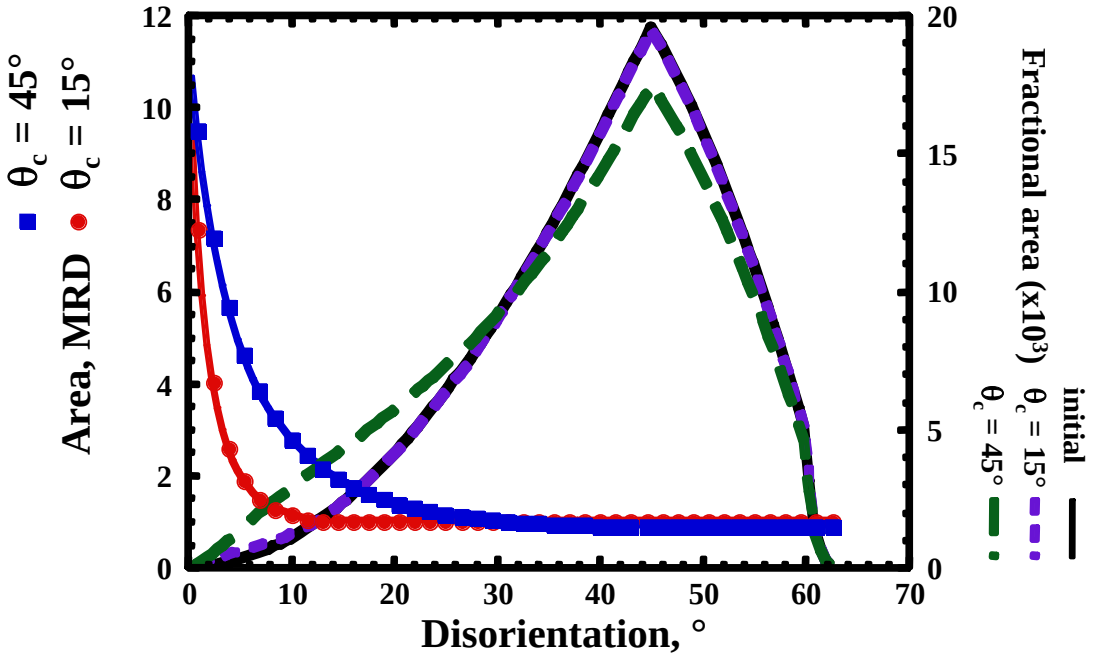

Figure 5. Steady state grain boundary character distributions resulting from two different energy functions, specified by Eq. 4. In this case, Eq. 7 was assumed to represent the relationship between the area and the energy.

Results for other energy functions led to similar results. For example, the energy function specified by Eq. 5 is plotted in Fig. 6, together with the initial and final area distribution for the case of ε = 0.4. As before, the steady state population is inversely related to the assumed grain boundary energy.

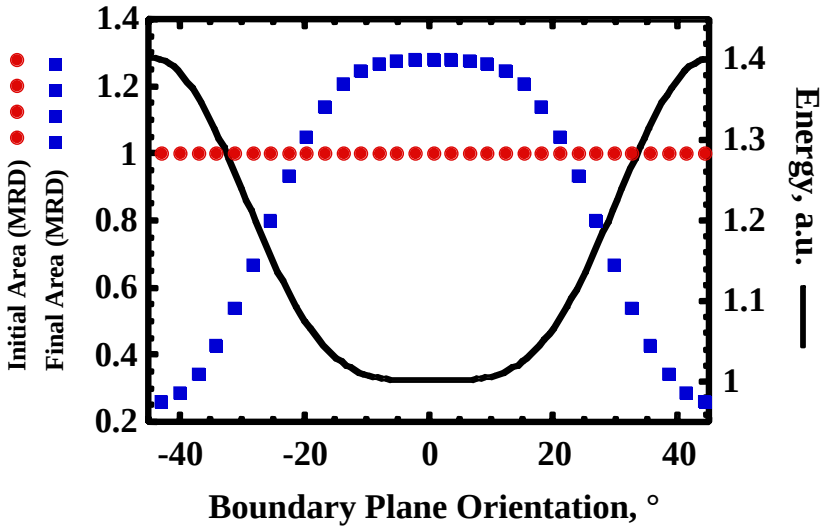

Figure 6. The initial and steady state GBCDs assuming the energy function specified in Eq. 5, for ε = 0.4. The energy function is also plotted.

As mentioned earlier, experiments and simulations show that the logarithm of the grain boundary population has an approximately inverse linear correlation with the grain boundary energy. As illustrated in Fig. 7, the relationship between the logarithm of the population determined by the critical event model and the energy is nearly linear over small ranges of energy anisotropy. However, for more realistic anisotropies, the slope of the $\ln(\lambda)$ v γ line decreases with γ.

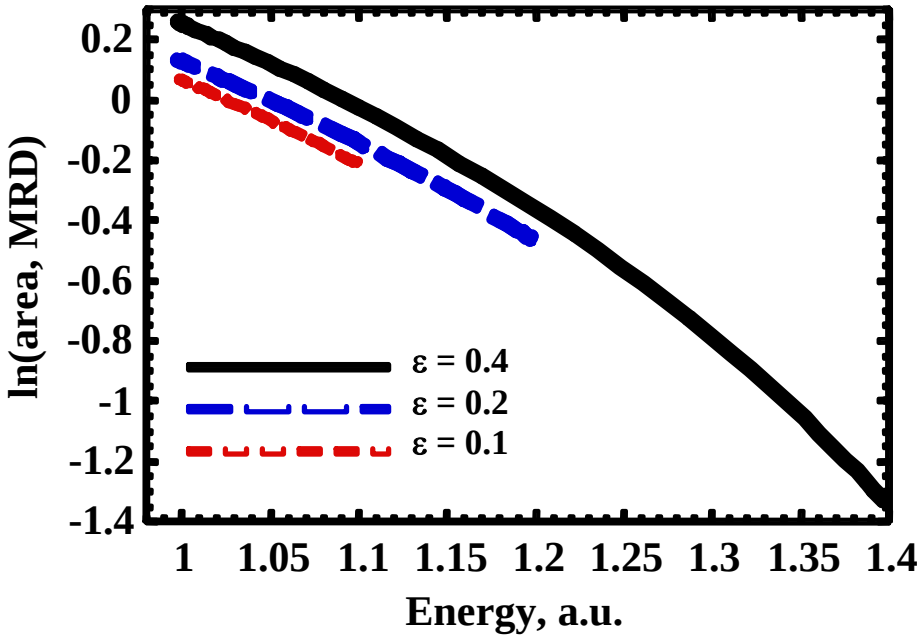

Figure 7. The logarithm of the steady state GBCD predicted by the critical event model for the energy function specified in Eq. 5, for three values of the amplitude, ε.

DISCUSSION

The model described here reproduces, qualitatively, the principal features observed in anisotropic grain boundary character distributions. First, it produces distributions in which both the numbers of low energy grain boundaries and the areas of these grain boundaries are enhanced. Second, it can produce MRD values greater than 3, as observed in real distributions. Finally, the logarithms of the areas of grain boundaries show an approximate inverse linear dependence on the grain boundary energy. The consistency between the observed distributions and those produced by the model indicates that the assumed mechanisms for the evolution of the distribution are plausible.

Additional work is required to make more quantitative comparisons to experiment. For example, the energy anisotropies have to have realistic ranges and exhibit variations over all crystallographic degrees of freedom. Of the energy anisotropies assumed in the present work, only the Read-Shockley energy the 15° cut-off is expected to be a reasonable approximation for the grain boundary energy anisotropy of cubic metals. However, the distribution that developed in response to this function is quite similar to the random distribution (see Fig. 3). While this difference might not be noticed in a typical experiment, it should be detectable. As part of our

future work, we plan careful experimental examinations of this part of the misorientation distribution.

While the model described here is successful in producing GBCDs that depend on the grain boundary energy anisotropy in a way that is consistent with experiment, the current form has limitations that will be addressed in future work. For example, the overall dissipation of grain boundary area is not addressed and the collapse of tetrahedral grains is not differentiated from the normal loss of faces. Furthermore, the energy anisotropies investigated to date depend on only a single crystallographic parameter. Also, in cases where there is an especially frequently occurring boundary type (for example, a twin), the GBCD will be influenced by the crystallographic constraints at the triple junctions and this in not accounted for in the current model [17]. Finally, the key to predictive accuracy for the model is the relationship between grain boundary energy and grain boundary area. While we believe that the relationship given by Eq. 2 is a reasonable approximation, it is assumed that the relationship derived from simulation (Eq. 7) is more accurate. At the current time, it is not known if this relationship will hold generally or if it will vary with the assumed energy anisotropy.

CONCLUSION

In conclusion, because of the constraint of interfacial equilibrium at triple lines, the average area of a given type of grain boundary is inversely related to its grain boundary energy. This area anisotropy affects the probabilities with which different grain boundary types are eliminated during grain growth, and this leads to anisotropy in the numbers of boundaries of different types. A simple model based on these principles predicts a relationship between grain boundary energy and the GBCD that is consistent with experimental observations.

ACKNOWLEDGEMENT

This work was supported primarily by the MRSEC program of the National Science Foundation under Award Number DMR-0520425

REFERENCES

[1]G.S. Rohrer, D.M. Saylor, B.S. El-Dasher, B.L. Adams, A.D. Rollett, P. Wynblatt, "The Distribution of Internal Interfaces in Polycrystals," *Z. Metall.* **95**, 197-214 (2004).

[2]D.M. Saylor, B.S. El-Dasher, T. Sano, G.S. Rohrer, "Distribution of Grain boundaries in $SrTiO_3$ as a Function of Five Macroscopic Parameters," *J. Amer. Ceram. Soc.* **87**, 670-76 (2004).

[3]D.M. Saylor, B.S. El Dasher, A.D. Rollett, G.S. Rohrer, "Distribution of Grain Boundaries in Aluminum as a Function of Five Macroscopic Parameters," *Acta Mater.* **52**, 3649-55 (2004).

[4]D.M. Saylor, A. Morawiec, G.S. Rohrer, , "Distribution of Grain boundaries in Magnesia as a Function of Five Macroscopic Parameters," *Acta Mater.* **51**, 3663-74 (2003).

[5]D.M. Saylor, A. Morawiec, G.S. Rohrer, "The Relative Free Energies of Grain boundaries in Magnesia as a Function of Five Macroscopic Parameters," *Acta Mater.* **51**, 3675-86 (2003).

[6]E.A. Holm, G.N. Hassold, and M.A. Miodownik, "On Misorientation Distribution Evolution During Anisotropic grain Growth," *Acta Mater.,* **49**, 2981-91 (2001).

[7]M. Upmanyu, G.N. Hassold, A Kazaryan, E.A. Holm, Y. Wang, B. Patton, D.J. Srolovitz, "Boundary Mobility and Energy Anisotropy Effects on Microstructural Evolution During Grain Growth," *Interface Science* **10**, 201-16 (2002).

[8]A. Kazaryan, Y. Wang, S.A. Dregia, an B.R. Patton, "Grain Growth in anisotropic systems: comparison of effects of energy and mobility," *Acta Mater.* **50** 2491-2502 (2002).

[9]D. Kinderlehrer, I. Livshits, G.S. Rohrer, S. Ta'asan, P. Yu, "Mesoscale Simulation of the Evolution of the Grain Boundary Character Distribution," *Mater. Sci. Forum* **467-470**, 1063-68 (2004).

[10]J. Gruber, D.C. George, A.P. Kuprat, G.S. Rohrer, A.D. Rollett, "Effect of Anisotropic Grain Boundary Properties on Grain Boundary Plane Distributions During Grain Growth," *Scripta Materialia* **53,** 351-355 (2005).

[11]G.S. Rohrer, "Influence of Interface Anisotropy on Grain Growth and Coarsening," *Annual Review of Materials Research* **35,** 99-126 (2005).

[12]C. DeW. Van Siclen, "Spatial correlation of high-energy grain boundaries in two-dimensional simulated polycrystal," *Acta Mater.* **55**, 983-9 (2007).

[13]F. Wakai, N. Enomoto, and H. Ogawa, "Three-dimensional microstructural evolution in ideal grain growth—general statistics,"Acta Mater. 48 (2002) 1297-1311.

[14]F.N. Rhines and B.R. Patterson, "Effect of the Degree of Prior Cold Work on the Grain Volume Distribution and the Rate of Gain Growth of Recrystallized Aluminum," *Mat. Trans.* **A13**, 985-993 (1982).

[15]J. Gruber, Ph.D. Thesis, Carnegie Mellon University, 2007.

[16]M. Miodownik, A.W. Godfrey, E.A. Holm, D.A. Hughes, "On boundary misorientation distribution functions and how to incorporate them into three-dimensional models of microstructural evolution," *Acta Mater.* **47**, 2661-68 (1999).

[17]C.S. Smith, in Metal Interfaces, ASM, Cleveland, OH, 1952, pp. 65-108.

[18]M. Frary, C.A. Schuh, "Connectivity and percolation behaviour of grain□boundary networks in three dimensions," *Phil. Mag.*, **85**, 1123-43 (2005).